

RESEARCH

Open Access



Multicellularity and increasing Reynolds number impact on the evolutionary shift in flash-induced ciliary response in Volvocales

Noriko Ueki^{1,2*} and Ken-ichi Wakabayashi^{2,3*}

Abstract

Background Volvocales in green algae have evolved by multicellularity of *Chlamydomonas*-like unicellular ancestor. Those with various cell numbers exist, such as unicellular *Chlamydomonas*, four-celled *Tetrabaena*, and *Volvox* species with different cell numbers (~1,000, ~5,000, and ~10,000). Each cell of these organisms shares two cilia and an eye-spot, which are used for swimming and photosensing. They are all freshwater microalgae but inhabit different fluid environments: unicellular species live in low Reynolds-number (Re) environments where viscous forces dominate, whereas multicellular species live in relatively higher Re where inertial forces become non-negligible. Despite significant changes in the physical environment, during the evolution of multicellularity, they maintained photobehaviors (i.e., photoshock and phototactic responses), which allows them to survive under changing light conditions.

Results In this study, we utilized high-speed imaging to observe flash-induced changes in the ciliary beating manner of 27 Volvocales strains. We classified flash-induced ciliary responses in Volvocales into four patterns: “1: temporal waveform conversion”, “2: no obvious response”, “3: pause in ciliary beating”, and “4: temporal changes in ciliary beating directions”. We found that which species exhibit which pattern depends on Re , which is associated with the individual size of each species rather than phylogenetic relationships.

Conclusions These results suggest that only organisms that acquired different patterns of ciliary responses survived the evolutionary transition to multicellularity with a greater number of cells while maintaining photobehaviors. This study highlights the significance of the Re as a selection pressure in evolution and offers insights for designing propulsion systems in biomimetic micromachines.

Keywords Volvocales, Multicellularity, Reynolds number, Cilia, Flagella

Background

In the history of evolution, multicellularity occurred multiple times independently; multicellularity is thought to result in survival advantages under selective pressure [1]. Multicellularity provides various benefits: avoiding predation due to larger size, effective predation/escape/movement to optimal environments due to faster moving speed, division of labor by cell differentiation, etc.

Volvocales green algae are a group of swimming phytoplankton that include species with a wide range of cell numbers, making them an excellent model for studying the evolution of multicellularity in existing organisms

*Correspondence:

Noriko Ueki

noriko.ueki@hosei.ac.jp

Ken-ichi Wakabayashi

kwakabayashi@cc.kyoto-su.ac.jp

¹ Science Research Center, Hosei University, Tokyo 102-8160, Japan

² Laboratory for Chemistry and Life Science, Institute of Innovative Research, Tokyo Institute of Technology, Yokohama 226-8501, Japan

³ Department of Industrial Life Sciences, Faculty of Life Sciences, Kyoto Sangyo University, Kyoto 603-8555, Japan



© The Author(s) 2024. **Open Access** This article is licensed under a Creative Commons Attribution-NonCommercial-NoDerivatives 4.0 International License, which permits any non-commercial use, sharing, distribution and reproduction in any medium or format, as long as you give appropriate credit to the original author(s) and the source, provide a link to the Creative Commons licence, and indicate if you modified the licensed material. You do not have permission under this licence to share adapted material derived from this article or parts of it. The images or other third party material in this article are included in the article's Creative Commons licence, unless indicated otherwise in a credit line to the material. If material is not included in the article's Creative Commons licence and your intended use is not permitted by statutory regulation or exceeds the permitted use, you will need to obtain permission directly from the copyright holder. To view a copy of this licence, visit <http://creativecommons.org/licenses/by-nc-nd/4.0/>.

(Fig. 1A and B). The multicellular species in Volvocales have either a flat or spherical shape. Flat species contain relatively few cells, like *Tetrabaena* and *Gonium* (Fig. 1A and C). Among spherical species, *Pandorina* has a morphology of densely packed cells, and those with more cells have a single layer of cells on the surface of the spheroid, like *Eudorina*, *Pleodorina*, and *Volvox* (Fig. 1A and C). Their evolution involved increasing complexity, such as in morphogenesis and sexual reproduction [2]. *Volvox*, which has the highest complexity, has the following survival advantage traits: they avoid predation by their large size [3, 4], swim fast [5], move quickly to optimum light environments [6], and differentiate between somatic and reproductive cells, with the reproductive cells being located and protected inside the spherical somatic cell sheet [7] (Fig. 1A).

With the increasing size of aquatic organisms, the physical properties of the surrounding fluid change. For organisms as small as 10 μm , such as *Chlamydomonas*, the environment is dominated by viscous forces. This would be like humans swimming in honey; thus, those small organisms must constantly generate propulsive forces to move. Cilia (or flagella) are considered adequate in such environments [12]. For smaller organisms $\sim 1 \mu\text{m}$ in diameter, such as *Escherichia coli*, the effect of diffusion by Brownian motion cannot be ignored. For larger ones, $> 1 \text{ mm}$, such as *Volvox* or *Daphnia*, the effect of inertia cannot be ignored [13, 14]. Accordingly, Volvocales range from sizes where viscous forces dominate to those with nonnegligible inertial forces. The ratio of inertia force to viscosity force is defined by the Reynolds number (Re), which is given by

$$Re = \frac{\rho VL}{\mu} = \frac{VL}{\nu}$$

where V (m/s) is the average velocity of an object relative to the fluid, L (m) is the characteristic length, ρ (kg/m^3) is the density of the fluid, μ ($\text{kg}/\text{m}\cdot\text{s}$) is the dynamic viscosity of the fluid, and ν (m^2/s) is the kinematic viscosity of the fluid. The equation above can be transformed as follows:

$$Re = \frac{\rho V^2}{\mu V/L}$$

where the numerator represents the inertia force, and the denominator represents the viscosity force. Thus, $Re > 1$ means that inertia overcomes viscosity.

Volvocales species commonly possess one eyespot and two cilia on each cell and beat the cilia toward the posterior of the individual with asymmetric waveforms consisting of effective and recovery strokes (Fig. 2A) [15]. Because the cilia deform differently during the

two strokes, propulsion is efficiently generated even in environments with low Re , i.e., where viscosity is dominant [16]. When the eyespot senses a light stimulus, the ciliary movement pattern alters, and Ca^{2+} influx into the cilia is considered to occur during this process [17].

Interestingly, several reports suggest that the regulation pattern in ciliary movement varies among species. In *Chlamydomonas reinhardtii*, the ciliary waveform converts from asymmetric to symmetric in response to a sudden increase in light intensity (such as flash illumination), causing temporal backward swimming called photoshock behavior (Fig. 2B) [20–24]. This waveform conversion is shared by other unicellular species of Volvocales, such as *Chlorogonium* and *Carteria*, and some prasinophytes, such as *Pyramimonas* and *Tetraselmis* [25]. In *Tetrabaena socialis*, which has a flat shape with four cells, cilia do not change their motility even after light stimulation, and no photobehavior is observed [19]. Several *Volvox* species temporarily reduce the ciliary beating frequency or stop ciliary movement in response to a sudden increase in light intensity [26, 27]. Other *Volvox* species in section *Volvox*, a group containing relatively more cells characterized by thick cytoplasmic bridges connecting cells, cilia temporarily change the direction of beating in response to sudden increase in light intensity while remaining in an asymmetric waveform (Fig. 2B) ([6] for *V. ferrisii* (previously reported as *V. rousseletii*); [27] for *V. barberi*). In both *Volvox* groups, those ciliary responses are considered to cause both phototactic and photoshock behaviors. A sudden increase in ambient light intensity induces a ciliary response in all cells throughout the sphere, causing photoshock behavior. When continuously illuminated from one direction, because of the self-rotation of the sphere about its anterior-posterior axis and directional photoreception at each eyespot, oscillation of light intensity is perceived by photoreceptors. In addition, cells closer to the anterior pole have larger eyespot. These factors result in a ciliary response only on the light side, whose amplitude is larger closer to the anterior pole, causing phototactic behavior (Fig. 2B) [6, 27–29].

Thus, Volvocales species commonly beat their cilia in an asymmetric waveform toward the backward of the individual during normal forward swimming; conversely, the responses of ciliary movement after a sudden change of light intensity differ among species. Here, the four patterns above are classified according to the number of cells and size of the individual as “1: temporal waveform conversion”, “2: no obvious response”, “3: pause in ciliary beating”, and “4: temporal changes in ciliary beating directions”. In this study, we categorized the pattern of ciliary response after a flash illumination is applied for 27

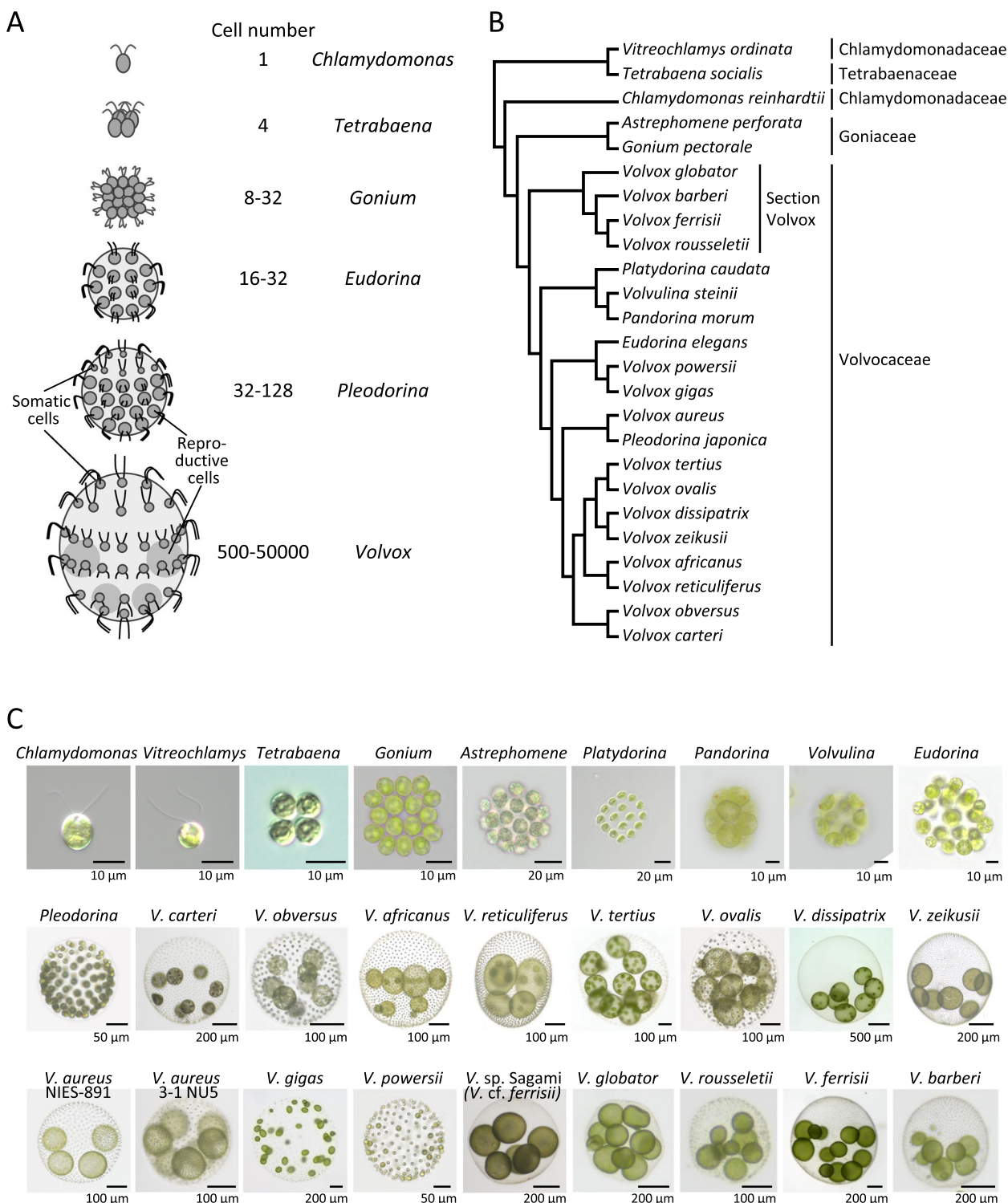


Fig. 1 Volvocales species/strains used in this study. **A** Schematic illustration of representative genera in Volvocales. **B** Phylogenetic relationships among the Volvocalean species examined in this study (Table 1). The cladogram was constructed based on the recent phylotranscriptomics/phylogenomics [8, 9] and the chloroplast multigene phylogeny [10] of homothallic *V. africanus* and *V. zeikusii*. Note that *Volvox ferrisii* includes *V. sp. Sagami* [11]. **C** Bright-field images of species/strains in Volvocales used in this study. Note the difference in scale bars. For species other than *Volvox*, only generic names are shown. For *Volvox*, abbreviated generic names and specific names are shown. See Table 1 for details

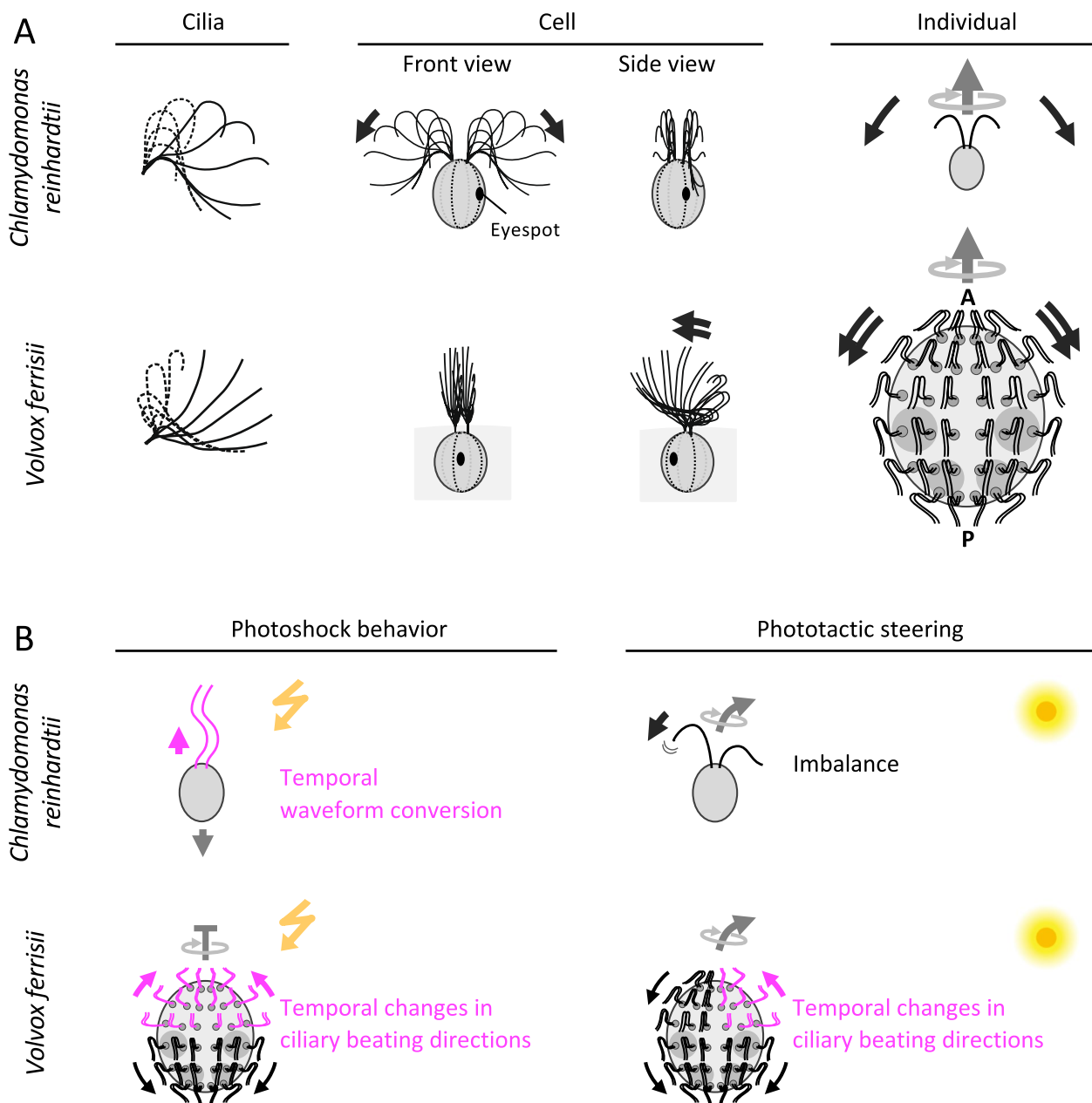


Fig. 2 Representative ciliary movements and photobehaviors in a unicellular and a multicellular species in Volvocales. **A** Ciliary and individual movement in *Chlamydomonas* and *Volvox*. Left: one stroke of an asymmetric waveform of cilia. Effective stroke (solid lines) and recovery stroke (broken lines) are shown. Modified by [6, 18]. Middle: Relationship between a cell and the direction of ciliary beating. Right: direction of the individual's forward swimming and rotation. Black arrows: direction of ciliary beating in the asymmetric waveform. Dark gray arrows: individual's swimming direction. Light gray arrows: direction of rotation. A, anterior pole; P, posterior pole. **B** Models of ciliary responses for photobehaviors in *Chlamydomonas reinhardtii* and *Volvox ferrisii* modified from [19]. The ciliary responses in magenta are focused on in this study

strains (Table 1, Fig. 1B and C) and found that the patterns matched better with the *Re* of each species than with phylogenetic relationships.

Materials and methods

Strains and cultural conditions

The Volvocales strains used in this study are listed in Table 1. *Chlamydomonas reinhardtii* strain CC-125 was grown in ~130 mL of tris-acetate-phosphate medium [30] in a 200-mL flask with aeration at 23°C

Table 1 Volvocales strains used in this study

Strain	Strain No. ^a
<i>Chlamydomonas reinhardtii</i>	CC-125
<i>Vitreochlamys ordinata</i>	NIES-882
<i>Tetrabaena socialis</i>	NIES-571
<i>Gonium pectorale</i>	Kaneko4 (=NIES-1711)
<i>Astrephomene perforata</i>	NIES-564
<i>Platydorina caudata</i>	NIES-728
<i>Pandorina morum</i>	NIES-574
<i>Volvolina steinii</i>	NIES-545
<i>Eudorina elegans</i>	UTEX 1193 (=NIES-717)
<i>Pleodorina japonica</i>	NIES-576
<i>Volvox carteri</i>	EVE10 (=UTEX1885)
<i>Volvox obversus</i>	UTEX 1865 (=NIES-868)
<i>Volvox africanus</i>	2013-0703-VO4 (=NIES-3780)
<i>Volvox reticuliferus</i>	VO123-F1-6 (=NIES-3785)
<i>Volvox tertius</i>	NIES-544
<i>Volvox ovalis</i>	UTEX RS12 (=NIES-2569)
<i>Volvox dissipatrix</i>	NIES-4270
<i>Volvox zeikusii</i>	NIES-731 ^b
<i>Volvox aureus</i>	NIES-891, 3-1 NU5
<i>Volvox gigas</i>	NIES-867
<i>Volvox powersii</i>	UTEX 1863 (=NIES-4127)
<i>Volvox</i> sp. Sagami (<i>V. cf. ferrisii</i> ^c)	NIES-4662
<i>Volvox globator</i>	SAG199.80 (=UTEX955)
<i>Volvox rousseletii</i>	UTEX 1862 (=NIES-734)
<i>Volvox ferrisii</i>	MI01 (=NIES-4029)
<i>Volvox barberi</i>	NIES-730

^a Strains indicated as "NIES-XXXX" were provided by the NIES through the NBRP of the MEXT, Japan

^b Reidentified [10]

^c See [11]

under continuous white, fluorescent light at $\sim 120 \mu\text{mol photons m}^{-2} \text{ s}^{-1}$. Other strains were grown in *Volvox* thiamin acetate (VTAC) medium [31, 32], except for *Tetrabaena socialis* in artificial freshwater-6 (AF-6) medium [31], statically in a test tube with a volume of 10 mL or in a 200-mL flask with a volume of ~ 130 mL at 24 °C–28 °C on a 16 h/8 h light/dark cycle under white fluorescent light at $\sim 120 \mu\text{mol photons m}^{-2} \text{ s}^{-1}$.

Observation of photo-induced ciliary response

Photo-induced ciliary responses were observed under a phase-contrast microscope (Axioscope 2, ZEISS or Axioscope 5, ZEISS) under red illumination (> 665 nm). Then, algae were stimulated by a white flash illumination (Speedlite 300EZ, Canon). The ciliary beating was video recorded at 500 frames per second using a high-speed CCD camera (HAS-U2, DITECT Corporation).

Character optimization

Parsimony was used for character optimization of patterns 1–4 in the “cladogram” (tree topology without tree length), with the general and simple optimization algorithms ACCTRAN (accelerated transformation) and DELTRAN (delayed transformation) [33], using PastML [34]. The cladogram of the species examined in this study (Table 1, Fig. 1) was constructed based on the recent phylotranscriptomics/phylogenomics [8, 9] and the chloroplast multigene phylogeny [10] of homothallic *V. africanus* and *V. zeikusii*. *V. sp.* Sagami (Table 1) was included in *V. ferrisii* [11].

Measurement of individual size and counting of cell number of individuals

Individuals of *Volvox* species were placed on a glass slide without a cover slip on top to avoid crushing or changing its size. They were photographed focusing on the periphery and surface of the spheroid using a stereomicroscope (Stemi508, ZEISS) equipped with a digital camera (WRAYCAM-NOA630B, Wraymer). The length in the anterior-posterior direction of the largest individual in the largest developmental stage was measured focusing on the periphery, and the number of somatic cells per area was counted focusing on the spherical surface; then, the total cell count was calculated. Species other than *Volvox* were photographed using a digital camera (Zeiss AxioCam 208 color) equipped with an optical microscope (Axioscope 5, ZEISS); the length in the anterior-posterior direction was measured, and the total cell number was counted in the largest individual.

Measurement of diameter and swimming speed and Reynolds-number calculation

About 8 mL of culture was placed into a 3.5 cm plastic petri dish (Iwaki) placed on the stage of a stereomicroscope (Stemi508, ZEISS) and video-recorded for around 1 min using an AxioCam 208 color camera (ZEISS). The distances that individuals traveled for 3–10 s were measured using the plugin “Manual Tracking” of FIJI (ImageJ) software version 2.1.0. Velocities were determined based on the time and distance traveled. The diameters of the individuals were measured in the direction perpendicular to the anterior-posterior axis using FIJI (ImageJ) software version 2.1.0, and approximated as the characteristic length for *Re*. The *Re* for each individual was calculated according to the following formula: diameter (μm) \times velocity ($\mu\text{m/s}$) / kinematic viscosity coefficient for water 10^6 ($\mu\text{m}^2/\text{s}$).

Results

Flash-induced ciliary responses could be categorized into four patterns in Volvocales

To understand the diversity of ciliary responses to a sudden increase in light intensity in Volvocales, we

observed ciliary movements after exposure to a white flash illumination in 27 strains (Table 1, Fig. 1B and C). The mode of flash-induced ciliary response was categorized into the following four patterns (summarized in Fig. 3E). Hereinafter, for readability, non-abbreviated generic names are shown for species other than *Volvox*.

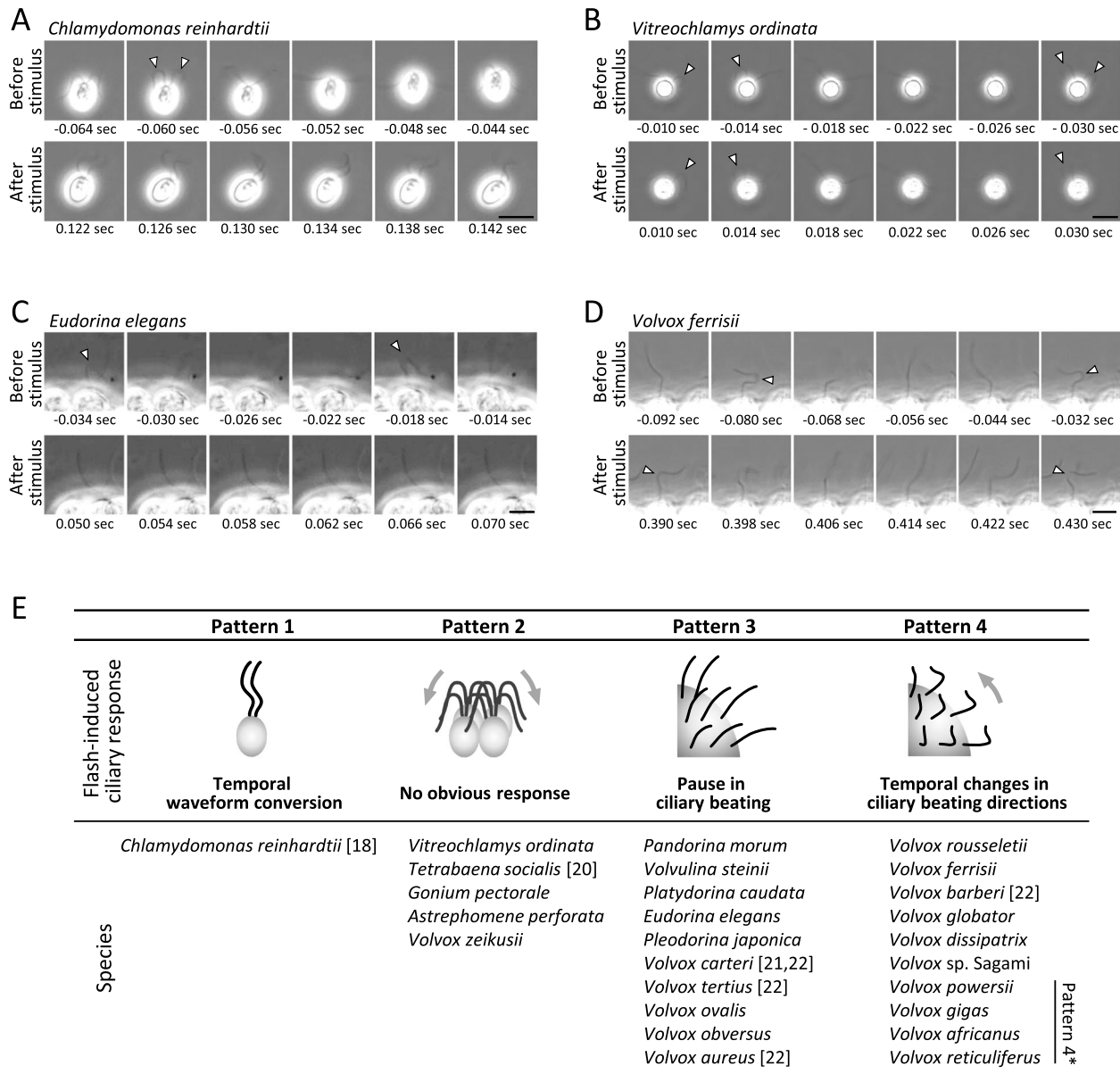


Fig. 3 Four patterns of flash-induced ciliary response. **A–D** Upper rows: sequential images at equal intervals covering > 1 stroke of the asymmetrical waveform before flash illumination. Bottom rows: sequential images after flashlight application in the same time interval as the upper rows. Time points from flash illumination are shown. White arrowheads indicate bends of asymmetric waveforms. **A** Temporal waveform conversion (Pattern 1) in *Chlamydomonas reinhardtii*. **B** No obvious response (Pattern 2) in *Vitreochlamys ordinata*. **C** A pause in ciliary beating (Pattern 3) in *Eudorina elegans*. **D** Temporal changes in ciliary beating directions (Pattern 4) in *Volvox ferrisii*. Scale bars: 10 μm. **E** Four patterns of flash-induced ciliary response. Volvocales species exhibiting each pattern are shown. An asterisk indicates species exhibiting both Patterns 3 and 4. Species with a citation ([#]) have already been reported on the pattern of ciliary responses similar to those observed in this study

Pattern 1: temporal waveform conversion

In the unicellular species *Chlamydomonas*, cilia transiently converted their waveform from asymmetric to symmetric immediately after the flash illumination (Fig. 3A and E and Movie S1). Only *Chlamydomonas* showed this pattern among the species examined.

Pattern 2: no obvious response

No obvious light response has been reported for *Tetrabaena* [19]. Here, three closely related species, unicellular *Vitreochlamys*, 8–16 cells *Gonium*, and 32–64 cells *Astrephomene*, did not obviously respond to the flash illumination (Fig. 3B and E and Movie S2). In *Vitreochlamys*, spontaneous conversion from asymmetric to symmetric waveforms was frequently observed independent of the flash illumination, as reported for *Tetrabaena* [19]. In addition, *V. zeikusii*, a lineage far apart from the small species above, did not respond to the flash illumination.

Pattern 3: pause in ciliary beating

Ten species (eleven strains) of Volvocales temporarily ceased ciliary movement in response to flash illumination (Fig. 3C and E and Movie S3). In addition, cells closer to the anterior pole of the individuals were more responsive (Movie S3). *Pandorina* and *Volvulina* showed relatively short cessations of around 0.05 s, while larger species, such as *Pleodorina*, showed rather long arrest durations (several seconds).

Pattern 4: temporal changes in ciliary beating directions

Relatively larger species exhibited temporal ciliary reversal or change in the beating direction of an asymmetric waveform, all of which are *Volvox* (Fig. 3D and E and Movie S4). Similar to the organisms that exhibit Pattern 3, the cells closer to the anterior pole were more responsive. All species of the section *Volvox* used in this study (*V. rousseletii*, *V. ferrisii*, *V. barberi*, *V. globator* and *Volvox* sp. Sagami; Fig. 1B) and *V. dissipatrix* which is sampled in Thailand with a maximum diameter greater than 2 mm [10] exhibited only this pattern. The response typically lasted for one to several seconds.

Even within the organisms classified to those exhibiting Pattern 4, the details of the responses were slightly different depending on whether they are inside or outside of the section *Volvox*. In species in the section *Volvox*, the asymmetric waveforms in the changed direction during the response were smaller in amplitude and more three-dimensional than the usual asymmetric waveforms, as previously reported [6]. The time lag between the flash application and the onset of the ciliary response was ~0.2 s in the section *Volvox*. In contrast, *V. dissipatrix*, a species outside of the section *Volvox*, the shape and the amplitude of asymmetric waveform during the response

were almost identical to those before flash illumination. The time lag between the flash application and the ciliary response was ~1.5 s, which is longer than that in species in the section *Volvox*.

In addition, several other species exhibited both Pattern 3 and Pattern 4, and we termed this pattern Pattern 4* (Fig. 3E). In *V. powersii*, *V. reticuliferus*, and *V. africanus*, both patterns were observed in different areas of an individual. In *V. gigas*, the ciliary movement stopped immediately after flash illumination, followed by beating with an asymmetric waveform that changed direction by about 90°, then returning to the original beating direction.

Flash-induced ciliary responses are not completely branch-dependent

The family Volvocaceae is distinguished from the other three families by its spherical shape and inversion during development. All strains in Volvocaceae exhibited Pattern 3 or 4, or both, except for *V. zeikusii* (Figs. 1B and 3E). All other families showed Pattern 1 or 2. Pattern 1 was observed only in the unicellular *Chlamydomonas*. Pattern 2 was observed in the unicellular *Vitreochlamys* and multicellular species in Tetrabaenaceae and Goniaceae. All species in section *Volvox* and *V. dissipatrix*, phylogenetically distant from section *Volvox*, showed only Pattern 4. *V. gigas* and *V. powersii*, and *V. africanus* and *V. reticuliferus*, which are closely related to each other, showed both Patterns 3 and 4 (Fig. 3E).

To deduce the character change of the four patterns during the evolution of the Volvocales, character optimization was performed. The species examined in this study included three species (*Volvox* sp. Sagami, homothallic *V. africanus* and *V. zeikusii*) that were not examined in the recent phylotranscriptomics/phylogenomics and ancestral state reconstructions in Volvocales [8, 9]. Thus, we can only show the tree topology of species examined in the present study by the “cladogram” without tree lengths. As already known from general textbooks (e.g. [33]), character optimization (ancestral state reconstruction) based on only tree topology is possible by parsimony and it is used for many studies of fossils [35, 36]. Therefore, we used parsimony for character optimization of patterns 1–4 in the “cladogram” (tree topology without tree length) (Fig. S1). Pattern 4 may have evolved at least three times independently within the Volvocaceae.

Relationship between cell number and size and patterns of photo-induced ciliary responses

The above data suggest that the patterns of photo-induced ciliary response are not solely dependent on lineage. We surmised that the number of cells in an individual and the size of the individual may be factors determining

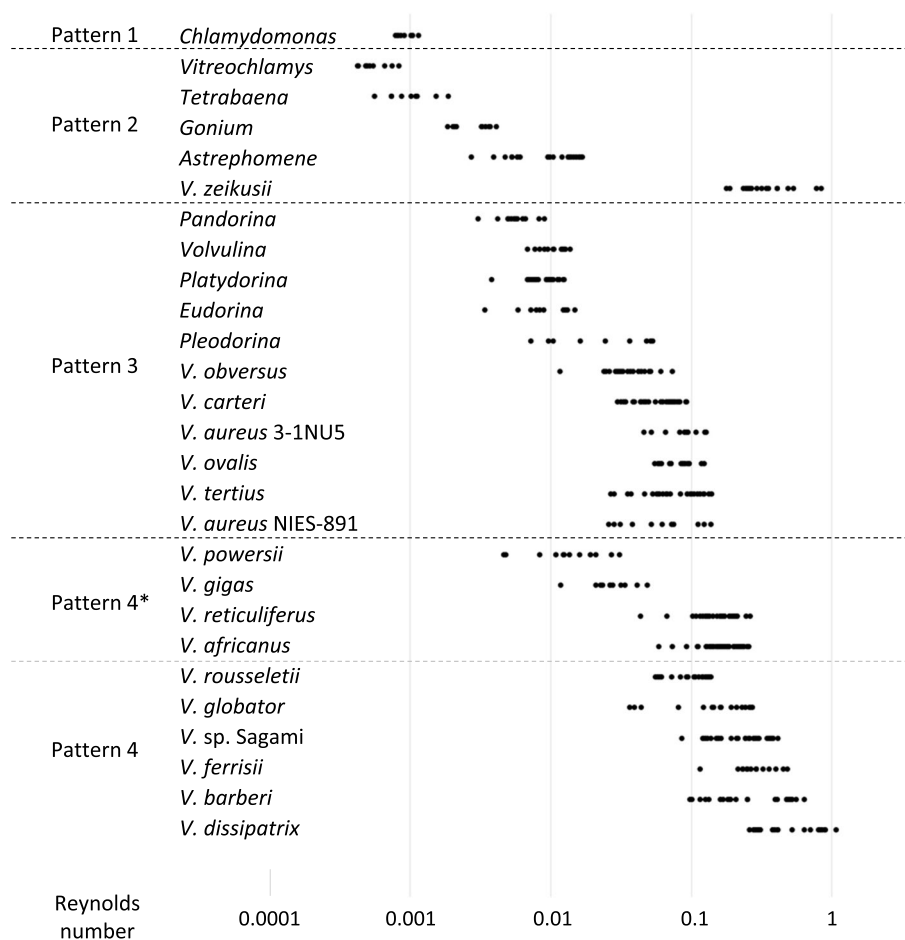


Fig. 5 Reynolds numbers of 27 strains in Volvocales for each pattern. Strains exhibiting Patterns 1 to 4 are listed from the top in order of decreasing Re within each pattern. Each dot derives from an individual

Chlamydomonas and has a chloroplast with high photoprotection ability [19, 37]. Having chloroplasts with high photoprotection ability is considered to be *Tetrabaena*'s strategy to avoid high-light stress, which contrasts with that of *Chlamydomonas*, which quickly escapes from light. The same strategy could be shared by species exhibiting Pattern 2.

Another possibility in species exhibiting Pattern 2 is that the threshold light intensity at which ciliary response occurs is significantly higher than the species exhibiting the other patterns. Stronger light stimuli than the camera strobe we used in this study should be tested.

After flash illumination, although both are unicellular, *Chlamydomonas* exhibited Pattern 1, waveform conversion, as previously reported [24], while *Vitreochlamys* did not respond obviously. *Vitreochlamys* may have different survival strategies from that of *Chlamydomonas*, e.g., gaining photoprotection ability like *Tetrabaena*. This idea should be confirmed by analyses of photosynthetic parameters in *Vitreochlamys*.

What we observed in this study is the flash-induced ciliary response, and Pattern 1 does not contribute to phototaxis; it induces a photoshock response in *Chlamydomonas* (Fig. 2B). Therefore, if an organism exhibits Pattern 2, it does not necessarily mean that the organism does not exhibit any photobehavior. In fact, among the species exhibiting Pattern 2, the ability of phototactic behavior varies; *Tetrabaena* has been reported to exhibit no phototaxis [19], and *Gonium* does [38]. It is possible that the abrupt change in light intensity used in this study does not trigger modification of ciliary movement in *Gonium*, but a smaller change in light intensity does induce phototaxis. Alternatively, changes in water flow around the colony of *Gonium* to induce phototaxis [38] may have occurred in response to flash illumination in our experiment, but the ciliary response for it was so slight that it could not be detected in our observation method.

Among large species with relatively high Re , only *V. zeikusii* exhibited Pattern 2 (Fig. 5). The circumstance that

V. zeikusii exhibits Pattern 2 and that for smaller species may be different. Curiously, *V. zeikusii* has been reported to have an exceptionally small eyespot [10]. It is possible that *V. zeikusii* exhibits Pattern 2 simply due to its low light sensitivity due to the small eyespot.

Cilia motility changed significantly with the evolution to Volvocaceae

Volvocaceae's Patterns 3 and 4, pause and direction change, are distinctly different from those shown by early-branched species in Volvocales. The following four-step changes might have occurred during the evolution to Volvocaceae. (1) The trait of cilia beating in symmetrical waveforms has been lost, because the trait was observed in the Pattern-1 species (in a flash-dependent manner), in the Pattern-2 species (independently from the light stimulus) (*Tetrabaena* [19] and *Vitreochlamys* (this study)), but not observed in species with Patterns 3 and 4. (2) Instead, new Patterns 3 and/or 4 are acquired. High intraciliary Ca^{2+} concentration is a plausible factor that induces a transient pause or direction change instead of the symmetric waveform [20, 39]. (3) The photoprotection ability at the same level as Pattern-2 species can be maintained. (4) The flash-induced ciliary response observed in this study was used as a factor to execute both photobehaviors, photoshock and phototactic behavior, inferring from the use of Pattern 4 demonstrated in *V. ferrisii* (Fig. 2B) [6].

Pleodorina exhibited a longer duration to recover from the response than *Pandorina* and *Volvolina* (see Results), suggesting that larger species have longer durations among the Pattern-3 species. However, because we focused on the patterns of flash-induced ciliary responses, the present experiment did not provide sufficient data on the duration times. Further analyses are needed to determine if this trend is general among the Pattern-3 species.

The direction-change pattern is related to an increase in Reynolds number associated with multicellularity

Volvocaceae species exhibited Pattern 3 and/or 4. It was indicated that Pattern 3 was an ancestral trait and Pattern 4 was a derived trait within Volvocaceae (Fig. S1). The transition from Pattern 3 to Pattern 4 seems to occur when the maximum cell number exceeds several thousand, and the maximum anterior-posterior length of individuals exceeds about 600 μm (Fig. 4). Pattern 4 species, which have a higher cell number and size also tended to have higher Re (Fig. 5). All species that exhibit only Pattern 4 showed a maximum $Re > 0.1$, reaching 1 in *V. dissipatrix*. At those Re , it is likely that the individual's movement could no longer be controlled by the ciliary pause of Pattern 3, due to increased inertia. Instead, it

appears that the movement is controlled by the direction change of Pattern 4, creating a water flow in the opposite direction.

The structure and mechanism in cilia that enable the alteration in the ciliary beating patterns remain unclear. Studies using detergent-extracted cell models or isolated cilia showed Pattern 1 in *Chlamydomonas* and Pattern 4 in *V. ferrisii* in demembrated ciliary axonemes by the addition of ATP and Ca^{2+} in vitro [20, 39]. This suggests the molecular mechanism that enables photo-induced ciliary responses exists in a detergent-insoluble fraction, such as ciliary axonemes. Microstructure in the axonemes, which would include proteins that regulate the activity of the motor protein dynein, may differ in the cilia of the four groups of organisms.

Prospects for the relationship between the ciliary response pattern and Re

In this study, we found a curious correlation between flash-induced ciliary response patterns and Re in organisms in Volvocales. However, we must admit that there are some limitations in interpreting the data obtained or the kind of the data.

First, we cannot distinguish between increases in the cell number and those in Re . Since all species with a large number of cells in Volvocales are spherical, and since the propulsive force per cell is considered almost the same, an increase in the number of cells almost directly implies an increase in Re . It is unclear if the pattern change occurred due to the increase in the cell number, those in Re , or even some other factors.

This issue would be resolved by analyzing the ciliary response of phylogenetically distant organisms from Volvocales. Changes in ciliary beating patterns in response to stimuli are observed in organisms with ciliary movements in general [40]. For example, a ciliate *Paramecium* exhibits Pattern 4 upon mechanical stimuli [41]. Interestingly, Re of *Paramecium* is estimated to be ~ 0.1 [14], which is the value of the transition from Pattern 3 to Pattern 4 (Fig. 5). Comparison with the ciliary responses occurring in organisms other than Volvocales, e.g., ciliates and mollusk larvae, will provide a detailed picture of the relationship between ciliary response and Re .

Second, our analysis focused on Re , but other hydrodynamic factors may also need to be discussed. For example, Peclet number (Pe), a ratio of the advective transport rate to the diffusive transport rate, has been discussed on nutrient uptake of *Volvox* during forward swimming [42, 43]. Attempts to classify flash-induced ciliary responses by Pe may also possibly provide interesting data.

Third, the data we have obtained in this study are based on quantified observations and not on experimental modification of the fluid environment. In the

previous study that discussed *Re* and phototaxis ability in *Volvox*, the authors discuss the relationship between the rotation frequency of *Volvox* and its phototaxis ability by experimentally increasing the solution viscosity [28]. We have also considered modifying the solution viscosity, but in the case of our experiments, this is technically difficult, as not only does the solution viscosity need to be increased but also decreased to verify whether the flash-induced ciliary response changes immediately with *Re*. Further research would be needed on experiments, at least to increase viscosity.

Conclusions

In conclusion, we found diverse regulatory mechanisms of cilia in closely related organisms in Volvocales, and this diversity could be explained by *Re*, which increased during the evolution of multicellularity. This study suggests the importance of fluid dynamics as a selection pressure and also provides useful information for the design of propulsion systems in biomimetic micromachines.

Supplementary Information

The online version contains supplementary material available at <https://doi.org/10.1186/s12862-024-02307-1>.

Supplementary Material 1: Fig. S1. Character evolution of four patterns of flash-induced ciliary responses in the Volvocales. The optimization was based on maximum parsimony with ACCTRAN and DELTRAN, using PastML [34]. The cladogram is based on [9] and [8], except for homothallic *V. africanus* and *V. zeikusii* [10]. Branch lengths do not indicate evolutionary distances. For four patterns, see Fig. 3E.

Supplementary Material 2: Movie S1. Movie for Fig. 2A, showing a *Chlamydomonas reinhardtii* cell photostimulated at 2.7 s from the start of the video. The movie is run at $\times 1/17$ speed.

Supplementary Material 3: Movie S2. Movie for Fig. 2B, showing a *Vitreochlamys ordinata* cell photostimulated at 7.1 s from the start of the video. The movie is run at $\times 1/17$ speed.

Supplementary Material 4: Movie S3. Movie for Fig. 2C, showing a *Eudorina elegans* spheroid photostimulated at 3.1 s from the start of the video. The arrows indicate the cilia shown in Fig. 2C. The movie is run at $\times 1/17$ speed.

Supplementary Material 5: Movie S4. Movie for Fig. 2D, showing a *Volvox ferrisii* partial spheroid near the anterior pole photostimulated at 4.9 s from the start of the video. The asterisk indicates the cell shown in Fig. 2D. The movie is run at $\times 1/17$ speed.

Acknowledgements

We are grateful to Dr. Hisayoshi Nozaki (Univ. Tokyo) for providing Volvocales strains and for critical suggestions about strain selection and culture and character optimization, Dr. Akira Noga (Chuo Univ.) for maintaining the algae culture, and Dr. Akira Kihara (Hosei Univ.) for help with microscope setup. We also thank the NIES collection for advice regarding culture.

Authors' contributions

N.U. designed the research, performed all the experiments, analyzed all the data, and wrote the manuscript. K.W. designed the research, aided in interpreting the data, and edited the manuscript. All authors read and approved the final manuscript.

Funding

This work was supported by Japan Society for the Promotion of Science KAKENHI Grants to NU (JP19K23758, JP21K06295) and KW (JP22H02642, JP22H05674, JP22H01440, JP23K22711, JP23K18136), by Ohsumi Frontier Science Foundation (2-G0008) to KW, and by Dynamic Alliance for Open Innovation Bridging Human, Environment and Materials to NU and KW.

Availability of data and materials

The data analyzed during the current study are available from the corresponding author (NU) on reasonable request.

Declarations

Ethics approval and consent to participate

Not applicable.

Consent for publication

Not applicable.

Competing interests

The authors declare no competing interests.

Received: 28 February 2024 Accepted: 5 September 2024

Published online: 14 September 2024

References

- Bonner JT. The origins of multicellularity. *Integr Biol Issues News Rev.* 1998;1(1):27–36.
- Umen JG. *Volvox* and volvocine green algae. *EvoDevo.* 2020;11:13.
- Herron MD, Borin JM, Boswell JC, Walker J, Chen I-CK, Knox CA, Boyd M, Rosenzweig F, Ratcliff WC. De novo origins of multicellularity in response to predation. *Sci Rep.* 2019;9(1):2328.
- Kirk DL. *Volvox*: a search for the molecular and genetic origins of multicellularity and cellular differentiation. Cambridge: Cambridge University Press; 1998.
- Solari CA, Michod RE, Goldstein RE. *Volvox barberi*, the fastest swimmer of the Volvocales (Chlorophyceae) 1. *J Phycol.* 2008;44(6):1395–8.
- Ueki N, Matsunaga S, Inouye I, Hallmann A. How 5000 independent rowers coordinate their strokes in order to row into the sunlight: phototaxis in the multicellular green alga *Volvox*. *BMC Biol.* 2010;8:103.
- Matt G, Umen J. *Volvox*: a simple algal model for embryogenesis, morphogenesis and cellular differentiation. *Dev Biol.* 2016;419(1):99–113.
- Lindsey CR, Knoll AH, Herron MD, Rosenzweig F. Fossil-calibrated molecular clock data enable reconstruction of steps leading to differentiated multicellularity and anisogamy in the Volvocine algae. *BMC Biol.* 2024;22(1):79.
- Ma X, Shi X, Wang Q, Zhao M, Zhang Z, Zhong B. A Reinvestigation of multiple independent evolution and Triassic-Jurassic origins of multicellular volvocine algae. *Genome Biol Evol.* 2023;15(8):evad142.
- Nozaki H, Takusagawa M, Matsuzaki R, Misumi O, Mahakham W, Kawachi M. Morphology, reproduction and taxonomy of *Volvox disipatrix* (Chlorophyceae) from Thailand, with a description of *Volvox zeikusii* sp. nov. *Phycologia.* 2019;58(2):192–9.
- Nozaki H, Ueki N, Isaka N, Saigo T, Yamamoto K, Matsuzaki R, Takahashi F, Wakabayashi K-I, Kawachi M. A new morphological type of *Volvox* from Japanese large lakes and recent divergence of this type and *V. ferrisii* in two different freshwater habitats. *PLoS One.* 2016;11(11):e0167148.
- Purcell E. Life at low Reynolds number. *Am J Phys.* 1977;45:3–11.
- Elgeti J, Winkler RG, Gompper G. Physics of microswimmers—single particle motion and collective behavior. *Rep Progs Phys.* 2015;78(5):056601.
- Lauga E, Powers TR. The hydrodynamics of swimming microorganisms. *Rep Prog Phys.* 2009;72(9):096601.
- Hoops H. Motility in the colonial and multicellular Volvocales: structure, function, and evolution. *Protoplasma.* 1997;199:99–112.

16. Sleight M. Mechanisms of flagellar propulsion: a biologist's view of the relation between structure, motion, and fluid mechanics. *Protoplasma*. 1991;164:45–53.
17. Kreimer G, Wakabayashi K-I, Hegemann P, Dieckmann C. The eyespot and behavioral light responses. In: *The Chlamydomonas Sourcebook*. 2023. p. 391–419.
18. Dutcher SK. Asymmetries in the cilia of *Chlamydomonas*. *Philos Trans R Soc Lond B Biol Sci*. 2020;375(1792):20190153.
19. Tanno A, Tokutsu R, Arakaki Y, Ueki N, Minagawa J, Yoshimura K, Hisabori T, Nozaki H, Wakabayashi K-I. The four-celled Volvocales green alga *Tetra-baena socialis* exhibits weak photobehavior and high-photoprotection ability. *PLoS One*. 2021;16(10):e0259138.
20. Bessen M, Fay RB, Witman GB. Calcium control of waveform in isolated flagellar axonemes of *Chlamydomonas*. *J Cell Biol*. 1980;86(2):446–55.
21. Brokaw C. Models for oscillation and bend propagation by flagella. In: *Symposia of the Society for Experimental Biology*. 1982. p. 313–338.
22. Hyams JS, Borisy GG. Isolated flagellar apparatus of *Chlamydomonas*: characterization of forward swimming and alteration of waveform and reversal of motion by calcium ions in vitro. *J Cell Sci*. 1978;33:235–53.
23. Schmidt JA, Eckert R. Calcium couples flagellar reversal to photostimulation in *Chlamydomonas reinhardtii*. *Nature*. 1976;262(5570):713–5.
24. Ringo DL. Flagellar motion and fine structure of the flagellar apparatus in *Chlamydomonas*. *J Cell Biol*. 1967;33(3):543–71.
25. Inouye I, Hori T. High-speed video analysis of the flagellar beat and swimming patterns of algae - possible evolutionary trends in green-algae. *Protoplasma*. 1991;164(1–3):54–69.
26. Sakaguchi H, Iwasa K. Two photophobic responses in *Volvox carteri*. *Plant Cell Physiol*. 1979;20(5):909–16.
27. Solari CA, Drescher K, Goldstein RE. The flagellar photoresponse in volvox species (volvocaceae, chlorophyceae)(1). *J Phycol*. 2011;47(3):580–3.
28. Drescher K, Goldstein RE, Tuval I. Fidelity of adaptive phototaxis. *P Natl Acad Sci USA*. 2010;107(25):11171–6.
29. Sakaguchi H, Tawada K. Temperature effect on photo-accumulation and phobic response of *Volvox aureus*. *J Protozool*. 1977;24(2):284–8.
30. Gorman DS, Levine RP. Cytochrome f and plastocyanin: their sequence in the photosynthetic electron transport chain of *Chlamydomonas reinhardtii*. *Proc Natl Acad Sci U S A*. 1965;54(6):1665–9.
31. Kasai F, Kawachi K, Erata M, Watanabe MM. NIES-collection list of strains. *Microalgae and protozoa*. *Res Rep NIES*. 2004;182:1–257.
32. Nozaki H, Kuroiwa H, Mita T, Kuroiwa T. *Pleodorina japonica* sp nov. (Volvocales, Chlorophyta) with bacteria-like endosymbionts. *Phycologia*. 1989;28(2):252–67.
33. Wiley EO, Brooks DR, Siegel-Causey D, Funk VA. *The complete cladist: a primer of phylogenetic procedures*. Lawrence: Natural History Museum, University of Kansas; 1991.
34. Ishikawa SA, Zhukova A, Iwasaki W, Gascuel O. A fast likelihood method to reconstruct and visualize ancestral scenarios. *Mol Biol Evol*. 2019;36(9):2069–85.
35. Forey P. Cladistics: optimisation. *Palaeontol Newsl*. 2006;63:26–35.
36. Jones ME, Benson RB, Skutschas P, Hill L, Panciroli E, Schmitt AD, Walsh SA, Evans SE. Middle Jurassic fossils document an early stage in salamander evolution. *Proc Natl Acad Sci*. 2022;119(30):e2114100119.
37. Arakaki Y, Kawai-Toyooka H, Hamamura Y, Higashiyama T, Noga A, Hirono M, Olson BJ, Nozaki H. The simplest integrated multicellular organism unveiled. *PLoS One*. 2013;8(12):e81641.
38. de Maleprade H, Moisy F, Ishikawa T, Goldstein RE. Motility and phototaxis of *Gonium*, the simplest differentiated colonial alga. *Phys Rev E*. 2020;101(2–1):022416.
39. Ueki N, Wakabayashi KI. Detergent-extracted *Volvox* model exhibits an anterior-posterior gradient in flagellar Ca(2+) sensitivity. *Proc Natl Acad Sci U S A*. 2018;115(5):E1061–8.
40. Inaba K. Calcium sensors of ciliary outer arm dynein: functions and phylogenetic considerations for eukaryotic evolution. *Cilia*. 2015;4(1):1–22.
41. Naito Y, Kaneko H. Reactivated triton-extracted models of paramecium: modification of ciliary movement by calcium ions. *Science*. 1972;176(34):523–4.
42. Solari CA, Ganguly S, Kessler JO, Michod RE, Goldstein RE. Multicellularity and the functional interdependence of motility and molecular transport. *Proc Natl Acad Sci*. 2006;103(5):1353–8.
43. Short MB, Solari CA, Ganguly S, Powers TR, Kessler JO, Goldstein RE. Flows driven by flagella of multicellular organisms enhance long-range molecular transport. *Proc Natl Acad Sci U S A*. 2006;103(22):8315–9.

Publisher's Note

Springer Nature remains neutral with regard to jurisdictional claims in published maps and institutional affiliations.